ac susceptibility and transport critical-current density of polycrystalline *c*-axis-oriented $YBa_2Cu_3O_{7-\delta}$ films: Josephson tunneling and *d*-wave pairing

W. Widder, L. Bauernfeind, and H. F. Braun
Experimentalphysik V, Universität Bayreuth, D-95440 Bayreuth, Germany

H. Burkhardt and D. Rainer
Theoretische Physik III, Universität Bayreuth, D-95440 Bayreuth, Germany

M. Bauer and H. Kinder
Institut für Festkörperphysik und Technische Physik, Technische Universität München, D-85747 Garching, Germany

(Received 3 May 1996)

We determined the intergranular critical-current density $j_{cJ}(T)$ of thin films of polycrystalline *c*-axis-oriented $YBa_2Cu_3O_{7-\delta}$ by measuring the isothermal ac susceptibility $\chi(h_{ac})$ at zero dc magnetic field. The temperature dependence of j_{cJ} was obtained from the temperature-dependent position of the intergrain peak in $\chi''(h_{ac})$. We confirmed our results by measurements of the transport critical current performed under self-field conditions. The observed temperature dependence of the critical current was compared with calculations of the Josephson critical current across rough interfaces. The experimental data can be explained by either assuming *d*-wave symmetry of the superconducting order parameter or, alternatively, by assuming *s*-wave symmetry and unusually strong pair breaking at the grain boundaries. The calculated critical currents show temperature dependences significantly different from the Ambegaokar-Baratoff formula, and agree well with recent measurements on single grain boundary junctions. [S0163-1829(97)02102-4]

I. INTRODUCTION

The symmetry of the superconducting order parameter reflects the nature of the mechanism that leads to the formation of Cooper pairs and constrains possible theories of high-temperature superconductivity. Recently, several experiments have been performed to investigate this symmetry (for an overview see, e.g., Refs. 1–3). There seems to be increasing evidence from these experiments that the superconducting order parameter has *d*-wave symmetry in high-temperature superconductors. Evidence for *d*-wave pairing comes, e.g., from the temperature dependence of the penetration depth,[4] angle-resolved photoemission spectroscopy,[5] and especially from quantum interference experiments.[6–9] On the other hand, there are experiments that suggest other symmetries[10] precipitating a controversy over the symmetry of the superconducting order parameter.

Superconducting states with anisotropic pairing (such as *d*-wave pairing) and isotropic pairing behave differently at surfaces and interfaces.[11] Elastic scattering at surfaces or interfaces will suppress an anisotropic order parameter to some degree but will not affect an isotropic order parameter. Hence, one expects to gain information on the anisotropy of the order parameter by measuring the effects of grain boundaries on superconducting properties. Polycrystalline high-temperature superconductors can be viewed as a network of individual superconducting grains which are separated by grain boundaries and coupled via Josephson junctions.[12] The presence of Josephson junctions affects the magnetic as well as the transport properties of such systems. Whereas the granularity of the samples manifests itself in reduced values of the transport critical current density, magnetic measurements, especially of the ac susceptibility of such samples, show both intragrain and intergrain characteristics.[13] (For further measurements concerning the temperature dependence of the critical current density of granular films and individual grain boundary junctions see, e.g., Refs. 14–16.) In a recent work on bulk $(Y_{1-x}Pr_x)Ba_2Cu_3O_{7-\delta}$ ceramic samples[17] we observed that the temperature dependence of the intergranular critical-current density resembles a behavior theoretically predicted for *d*-wave superconductors by Xu *et al.*[18] This anomalous temperature dependence is traditionally interpreted in terms of flux creep.[19] On the other hand, the striking agreement between the temperature dependence measured on granular (misoriented) bulk samples and the theory of Xu *et al.* has been interpreted in Ref. 17 as evidence for *d*-wave pairing.

To make the comparison between theory and experiment more precise, we have investigated *c*-axis-oriented polycrystalline $YBa_2Cu_3O_{7-\delta}$ (YBCO) films and interpreted our results using a model beyond the tunneling Hamiltonian approach.[20] Our calculations include an interface barrier, interface roughness, and the suppression of the order parameter associated with an interface. We find good agreement of the observed temperature dependence of the critical current and the model calculations, which we consider as an indication of pair breaking effects at the grain boundary. Such pair breaking effects are a natural consequence of anisotropic *d*-wave pairing. For *s*-wave pairing such pair breaking effects can arise from, e.g., magnetic scattering.

The experiments on *c*-axis-oriented YBCO films are described in Secs. II and III. Their theoretical interpretation is presented in Sec. IV, and the results are summarized in Sec. V.

II. EXPERIMENTAL DETAILS

Polycrystalline c-axis-oriented $YBa_2Cu_3O_{7-\delta}$ thin films were deposited on polished Y_2O_3-stabilized ZrO_2 substrates using thermal coevaporation. The deposition chamber is described in detail elsewhere.[21] The substrate temperature was 680–700 °C and the oxygen pressure near the substrate was 0.002 mbar. To obtain c-axis-oriented YBCO films, we deposited a 50-nm-thick buffer layer of amorphous YBCO at a substrate temperature of only 400 °C. The substrate temperature was then increased and the polycrystalline YBCO film was grown.[22]

The degree of misorientation of the c-axis-oriented grains was determined from rocking curves which have been performed on a Seifert XRD 3000 P diffractometer (Cu $K\alpha$ radiation). Scanning electron microscopy (SEM) images were used to determine the morphology of the grains and the porosity of the samples. Magnetic measurements were performed in a homemade susceptometer using a standard lock-in technique. The complex susceptibility of square-shaped samples with dimensions 2.5×2.5 mm^2 cut from a 1×1 cm^2 parent film was measured at 1111 Hz as a function of the field amplitude h_{ac} ($0.014\ \mathrm{G}\leqslant h_{ac}\leqslant 18.4\ \mathrm{G}$) at constant temperature. The orientation of the ac field h_{ac} was perpendicular to the film surface, i.e., parallel to the c axis of the microcrystals. Transport critical currents were measured using a standard four-point method. The sample for these experiments was cut from the same parent specimen as was taken for the susceptibility measurements. The bridge (0.9×0.5 mm^2) in the middle of the striplike sample (8×2 mm^2) was patterned by carefully removing parts of the YBCO film with the help of a diamond file. The transport intergranular critical-current density j_{cJ} of the film was obtained by dividing the critical current of the patterned sample by the cross section of the constricted area. The current contacts were made of annealed gold foil and they were fixed to the sample with silver paint. For the voltage contacts, we used silver wires which also were initially annealed and attached to the sample with silver paint. The electric field criterion used was 3 μV/cm.

III. EXPERIMENTAL RESULTS

A. Sample characterization

The x-ray-diffraction pattern for the polycrystalline c-axis-oriented $YBa_2Cu_3O_{7-\delta}$ film is shown in Fig. 1. The c-axis orientation of the grains is confirmed by the diffraction profile which predominantly exhibits ($00l$) peaks. Peaks which result from the substrate are marked with an ''S.'' The (200) peak is caused from small amounts of a-axis-oriented grains. The degree of misorientation of the c-axis-oriented grains was determined from rocking curves. Figure 2 displays as an example the rocking curve of the (005) peak. The full width at half maximum (FWHM) of the (003), (005), and (006) rocking curve was FWHM $\approx 4.8^{\circ}$. The morphology, and the size of individual grains as well as the porosity of the sample were analyzed from SEM images; an example is shown in Fig. 3. The diameter of the platelike grains is ≈ 0.5 μm. A few a-axis-oriented grains can be seen as bright ''sticks.'' The temperature-dependent resistivity of our sample is shown in Fig. 4. Since the best single crystal-

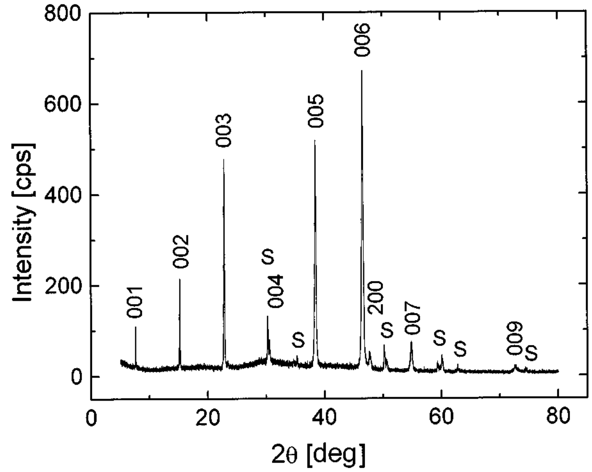

FIG. 1. X-ray-diffraction pattern of a polycrystalline c-axis-oriented $YBa_2Cu_3O_{7-\delta}$ film. The peaks coming from the substrate are indicated with an ''S.''

line $YBa_2Cu_3O_{7-\delta}$ films have $\varrho_{ab}(T)\approx 0.6$ $\mu\Omega$ cm $\times T$[K] above 100 K,[23] the large resistivity of our sample is caused from an increased resistivity of the intergrain layers. This can be understood by simply modeling our sample as square arrangement of 0.5×0.5 μm^2 large superconducting grains which are separated by a 10-Å-thick intermediate layer. Using this model we obtain for the intermediate layer $\varrho\approx 0.3$ Ω cm at $T=100$ K which is a typical value for a semiconductor. Gross and Mayer[24] observed similar values for the normal resistivities ($\varrho\approx 0.1-1$ Ω cm) of single grain boundary junctions.

B. Isothermal field-dependent ac susceptibility measurements and transport critical-current measurements

To investigate the temperature dependence of the intergranular critical current density $j_{cJ}(T)$ of the polycrystalline c-axis-oriented $YBa_2Cu_3O_{7-\delta}$ thin film, isothermal field-dependent ac susceptibility measurements $\chi(h_{ac})$ have been performed at zero dc magnetic field. The imaginary part of the susceptibility $\chi''(h_{ac})$ exhibits two maxima as can be seen in Fig. 5 for $T=74$ K. The low-field maximum at h_{ac}^{J} is

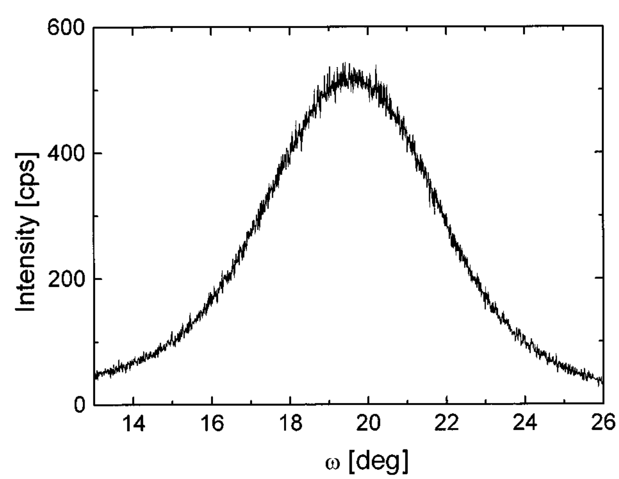

FIG. 2. Rocking curve of the (005) peak.

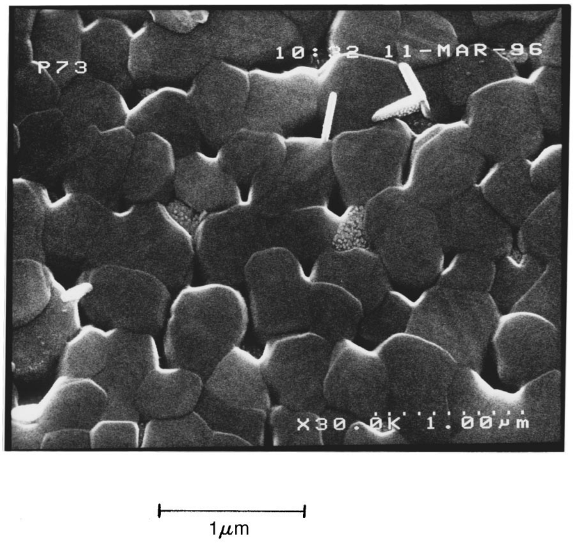

FIG. 3. SEM image from a part of the polycrystalline c-axis-oriented $YBa_2Cu_3O_{7-\delta}$ film.

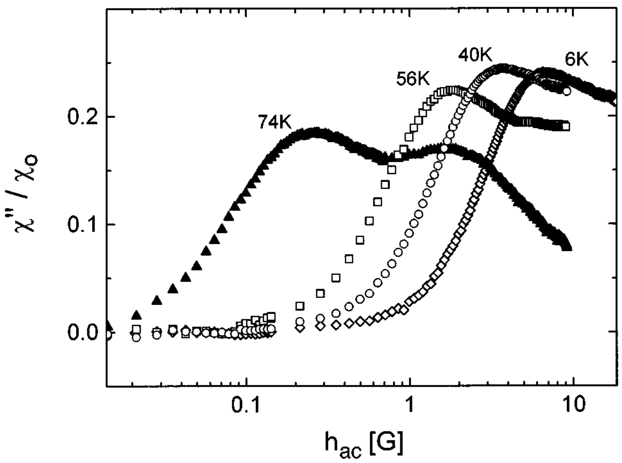

FIG. 5. Field dependence of the imaginary part $\chi''(h_{ac})$ of the complex susceptibility $\chi(h_{ac})$ at T = 6, 40, 56, and 74 K for the polycrystalline c-axis-oriented $YBa_2Cu_3O_{7-\delta}$ film.

caused by intergrain losses, whereas the high-field maximum at h_{ac}^G is related to intragrain losses. Both of these maxima shift to higher field amplitudes with decreasing temperature (therefore in our case the intragrain maximum cannot be seen for the lower temperatures of Fig. 5).

For a thin superconducting disk and small perpendicular applied ac fields h_{ac}, Clem and Sanchez[25] obtained the following limiting behavior for the fundamental component of the ac susceptibility:

$$\chi'(h_{ac}) \approx -\chi_0\left(1-\frac{15h_{ac}^2}{32h_d^2}\right), \quad h_{ac} \ll h_d, \tag{1}$$

$$\chi''(h_{ac}) \approx \chi_0 \frac{h_{ac}^2}{\pi h_d^2}, \quad h_{ac} \ll h_d. \tag{2}$$

Here $h_d = j_c d/2$ is a characteristic field for a disk-shaped sample, d is the thickness of the disk, $\chi_0 = 8R/3\pi d$, R is the radius of the disk, and j_c has been assumed to be independent of field (Bean approximation[26]). From numerical calculations they found that the peak in χ'' occurs at $h_{ac} = 1.942 h_d$ where $\chi''_{max}/\chi_0 = 0.241$. Brandt showed that the difference in the ac response of a disk-shaped sample as opposed to our square-shaped sample is less than 1% and can be neglected.[27]

Thus the intergranular critical-current density for any temperature is given by the position of the maximum h_{ac}^J in $\chi''(h_{ac})$:

$$j_{cJ}(T) = \frac{h_{ac}^J(T)}{1.942 d/2}. \tag{3}$$

Figure 6 shows the temperature dependence of $j_{cJ}(T)$ obtained from Eq. (3). For temperatures below 60 K the measured values $\chi''_{max}/\chi_0 \approx 0.22$–$0.25$ (see Fig. 5) are in good agreement with Clem's calculation $\chi''_{max}/\chi_0 = 0.241$, which confirms the validity of the assumed Bean approximation.

In addition, we have performed transport critical-current measurements to confirm the inductively obtained temperature dependence of $j_{cJ}(T)$. We find the temperature depen-

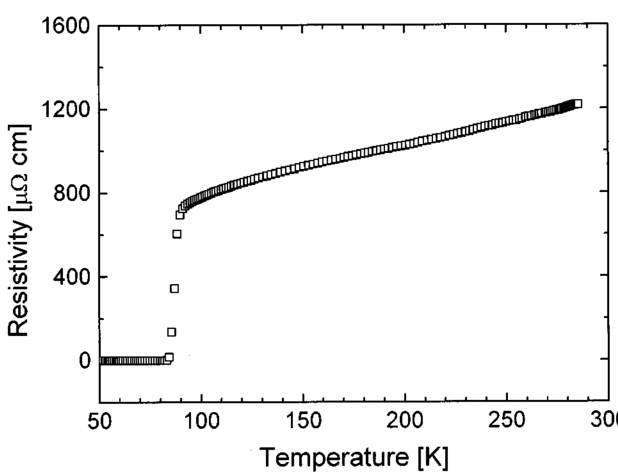

FIG. 4. Temperature dependence of the resistivity of the polycrystalline c-axis-oriented $YBa_2Cu_3O_{7-\delta}$ film.

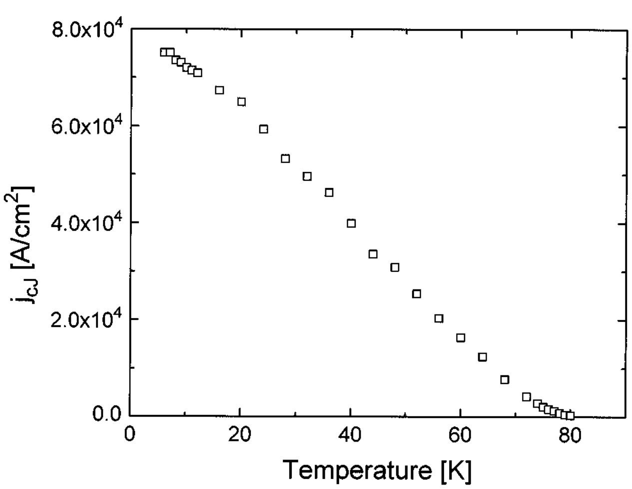

FIG. 6. Temperature dependence of the intergranular critical-current density $j_{cJ}(T)$ for the polycrystalline c-axis-oriented $YBa_2Cu_3O_{7-\delta}$ film as determined from $\chi''(h_{ac})$ measurements.

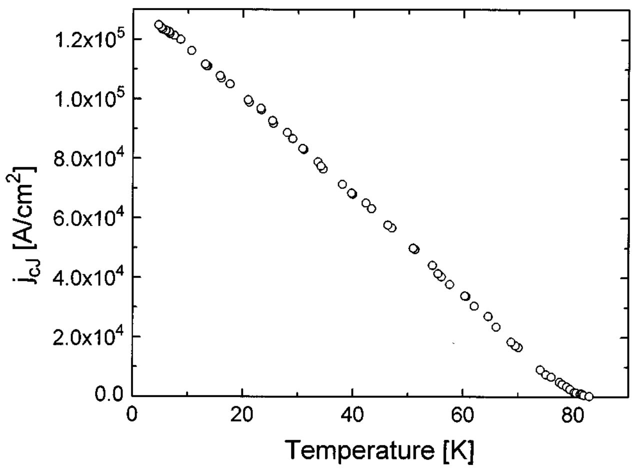

FIG. 7. Temperature dependence of the intergranular critical-current density $j_{cJ}(T)$ for the polycrystalline c-axis-oriented $YBa_2Cu_3O_{7-\delta}$ film as determined from transport measurements.

dence shown in Fig. 7. Although these resistively obtained values are about a factor of 1.6 larger than those obtained inductively, both methods yield temperature dependences that are in quite good agreement. This can be seen in Fig. 10, below, where we have plotted the normalized intergranular critical current density $j_{cJ}(T)/j_{cJ}(0)$ of the polycrystalline c-axis-oriented $YBa_2Cu_3O_{7-\delta}$ film as determined inductively (□) and resistively (○). Also included in Fig. 10 is the inductively obtained temperature dependence $j_{cJ}(T)/j_{cJ}(0)$ of a second film (△) which has been covered *ex situ* with several nm of $LaAlO_3$. As can be seen in Fig. 10 this protective layer does not influence the temperature dependence of j_{cJ}. The solid, dashed, and dotted lines are the result of a theoretical analysis described below.

IV. THEORETICAL INTERPRETATION

The theory of Josephson weak links together with strong pair breaking effects associated with interfaces between grains provides an excellent description of our data. For an anisotropic superconductor, interface roughness is a natural pair breaking mechanism. On the other hand (see below), unusually large pair breaking scattering rates associated with the interface (e.g., inelastic scattering or magnetic scattering) are required to obtain the same agreement for an isotropic ''s-wave'' superconductor. Our approach differs fundamentally from models in which the critical current is determined by flux motion.[19]

We will model our granular films in the following as a network of superconducting-insulating-superconducting (SIS) junctions, because there is increasing evidence that the boundaries between superconducting grains in polycrystalline $YBa_2Cu_3O_{7-\delta}$ are insulating and not metallic. The following arguments support this picture.

(1) Apart from the Y-123 phase there are no metallic phases in the Y_2O_3-BaO-CuO-phase diagram.

(2) Transmission electron microscopy (TEM) images of polycrystalline Y-123 samples show no evidence for chemical segregation at grain boundaries.[28] Thus the formation of metallic impurity phases by chemical segregation at the grain boundaries appears to be unlikely.

(3) An amorphous zone at the grain boundaries results from the strain associated with an increased dislocation density at the boundaries.[28,29] The cores of these grain boundary dislocations are believed to suppress the superconducting order parameter. In addition, oxygen-annealing experiments provide evidence that the interface layers between adjacent grains are oxygen deficient.[30] Both oxygen disorder and oxygen deficiency lead to a decrease of T_c and ultimately to insulating behavior.

(4) The normal resistances obtained for single grain boundary junctions are typical for semiconductors and significantly larger than the values for metallic interface layers.[24]

(5) The observation of electromagnetic resonances along a YBCO bicrystal grain boundary junction gives further evidence that the grain boundary is insulating.[31,32]

We focus first on a single SIS junction. The critical current of Josephson junctions was calculated by Ambegaokar and Baratoff.[33] They considered isotropic superconductors and established the following universal formula for a SIS Josephson junction:

$$I_c(T)=\frac{\pi}{2eR_N}\Delta(T)\tanh\frac{\Delta(T)}{2k_BT}. \tag{4}$$

The temperature dependence and magnitude of the critical current are determined in this theory by the BCS energy gap $\Delta(T)$ and the normal state resistance R_N of the junction. The corresponding formula[34] for anisotropic superconductors is given by

$$I(T,\psi)=4eN_f^lN_f^rk_BT \times\sum_{\epsilon_n}\text{Im}\left\langle\left\langle|T_{\vec{p}_f^l\vec{p}_f^r}|^2\frac{\pi\Delta^l(\vec{p}_f^l)}{\sqrt{\epsilon_n^2+|\Delta^l(\vec{p}_f^l)|^2}} \times\frac{\pi(\Delta^r(\vec{p}_f^r))^*\exp(i\psi)}{\sqrt{\epsilon_n^2+|\Delta^r(\vec{p}_f^r)|^2}}\right\rangle_{\vec{p}_f^l}\right\rangle_{\vec{p}_f^r}, \tag{5}$$

where ψ is the phase difference across the junction. The critical current is obtained as the maximum Josephson current, $I_c(T)=\max_{\{\psi\}}I(T,\psi)$. Here, N_f^l (N_f^r), $\vec{p}_f^l$ ($\vec{p}_f^r$), and Δ^l (Δ^r) are the density of states, the Fermi momenta, and the momentum-dependent order parameters of the superconductors on the left (right) sides of the junction, $\epsilon_n=(2n+1)\pi k_BT$ are the Matsubara energies, and $\langle\cdots\rangle_{\vec{p}_f^{l,r}}$ means averaging over the Fermi surfaces. The temperature dependence obtained from Eq. (5) is no longer universal but generally depends on the gap anisotropy, the anisotropy of the Fermi surface, and the exact form of the tunneling matrix elements $T_{\vec{p}_f^l\vec{p}_f^r}$. The magnitude $|T_{\vec{p}_f^l\vec{p}_f^r}|^2$ is the probability for a quasiparticle (in the normal state) to tunnel from state $\vec{p}_f^l$ on the left side of the junction to state $\vec{p}_f^r$ on the right side. Equation (5) does not reproduce the observed anomalies in the critical currents across grain boundaries. The resulting temperature dependence obtained from Eq. (5) is not very sensitive to d-wave pairing or anisotropies of the Fermi surface,[35] and $I_c(T)/I_c(0)$ deviates only slightly from the Ambegaokar-Baratoff result. Only the overall magnitude of the critical currents might be sensitive to details of the tunneling probabilities, the anisotropy of the order parameter, or the orientation of the grains. For example, formula (5) gives zero critical current for d-wave superconductors and isotropic tunneling probabilities.

We note that the derivation of Eq. (5) requires the assumption that the order parameter is not affected by the presence of the Josephson contact and keeps its bulk value up to the interface. This assumption breaks down for strongly anisotropic superconductors, such as d-wave superconductors, and the depletion of the order parameter leads to the observed anomalous temperature dependences (see below).

Self-consistent calculations of the spatial dependence of the order parameter show[36,37] that the gap amplitude of a d-wave superconductor is, in general, strongly suppressed near a surface or interface, as a consequence of quasiparticles reflecting from the surface (interface). Recently, Barash *et al.* [38] considered the case of two d-wave superconductors separated by a weakly transparent smooth interface.[39] They showed that the Josephson current depends in a nontrivial way on the order parameter up to distances from the barrier of the order ξ_0 where $\xi_0 = \hbar v_f / 2\pi k_B T_c$ is the zero-temperature coherence length. We use here the quasiclassical theory to calculate the distortion of the order parameter. With this input we calculate the Josephson current density $j(T,\psi)$ and the critical-current density $j_c(T)$. We will sketch our scheme for calculating $j_c(T)$ only briefly. Details of the calculations will be published elsewhere.[35]

A. Quasiclassical equations

The quasiclassical theory of superconductivity was developed by Eilenberger,[40] and Larkin and Ovchinnikov.[41] The theory is conveniently formulated in terms of the quasiclassical matrix propagator $\hat{g}(\vec{p}_f,\vec{R};\epsilon_n)$, which is a 2×2 matrix. Its diagonal terms carry the information on supercurrents and other measurable quantities of interest, whereas the off-diagonal part $\hat{f}(\vec{p}_f,\vec{R};\epsilon_n)$ determines the order-parameter matrix $\hat{\Delta}(\vec{p}_f,\vec{R})$. The quasiclassical propagator can be calculated from Eilenberger's differential equation

$$[i\epsilon_n\hat{\tau}_3 - \hat{\Delta}(\vec{p}_f,\vec{R}),\hat{g}(\vec{p}_f,\vec{R};\epsilon_n)] + i\hbar\vec{v}_f\cdot\vec{\nabla}_{\vec{R}}\hat{g}(\vec{p}_f,\vec{R};\epsilon_n) = 0, \tag{6}$$

which couples the diagonal and off-diagonal parts of $\hat{g}$. The coupling is provided by the order-parameter matrix $\hat{\Delta}$, which must be calculated self-consistently from the off-diagonal quasiclassical propagator via the gap equation

$$\hat{\Delta}(\vec{p}_f,\vec{R}) = k_B T \sum_{\epsilon_n}^{\epsilon_c} \langle V(\vec{p}_f,\vec{p}_f{}')\hat{f}(\vec{p}_f{}',\vec{R};\epsilon_n)\rangle_{\vec{p}_f{}'}. \tag{7}$$

Here, $\hat{\tau}_3$ is a Pauli matrix in particle-hole space, $\vec{p}_f$ and $\vec{v}_f$ are the Fermi momentum and Fermi velocity, and $\vec{R}$ is the spatial coordinate. We will use here an isotropic two-dimensional model for the conduction electrons, i.e., a cylindrical Fermi surface with radius p_f, an isotropic Fermi velocity $\vec{v}_f$, and a constant density of states N_f. The calculation of $\hat{\Delta}(\vec{p}_f,\vec{R})$ involves the pairing interaction $V(\vec{p}_f,\vec{p}_f{}')$ which we write in the case of a d-wave superconductor $[\Delta(\vec{p}_f) = \Delta\cos(2\phi)]$ as

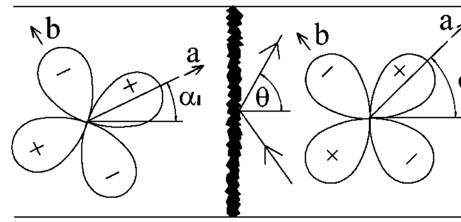

FIG. 8. Schematic geometry of our model for a grain boundary. The clover-shaped d-wave order parameter is fixed to the crystal lattice. The trajectory of an incoming quasiparticle is specified by the angle θ. The angles α_l and α_r are defined as the angles between the normal of the interface and the crystal lattice on the left and right sides, respectively.

$$V(\vec{p}_f,\vec{p}_f{}') = 2V_0\cos(2\phi)\cos(2\phi'). \tag{8}$$

The angles ϕ and ϕ' are the polar angles of the momenta $\vec{p}_f$ and $\vec{p}_f{}'$. For isotropic pairing we have $V(\vec{p}_f,\vec{p}_f{}') = V_0$. The critical temperature is determined by the coupling constant V_0 and the cutoff energy ϵ_c via the BCS relation $k_B T_c = 1.13\epsilon_c e^{-1/V_0}$. We are in particular interested in the superconducting current density, given in terms of $\hat{g}$ by

$$\vec{j}(\vec{R}) = 2eN_f k_B T \sum_{\epsilon_n} \langle \vec{v}_f \tfrac{1}{2}\mathrm{Tr}[\hat{\tau}_3\hat{g}(\vec{p}_f,\vec{R};\epsilon_n)]\rangle_{\vec{p}_f}. \tag{9}$$

B. Model for a grain boundary

Interfaces enter into the quasiclassical theory as boundary conditions connecting the quasiclassical propagators across the interface.[42–46] Zaitsev[42] was the first to derive the boundary condition for a smooth interface with reflection probability R. We use Zaitsev's boundary condition to describe the "smooth part" of grain boundary scattering. The reflection probability depends on the angle of incidence θ of a quasiparticle (for a definition of the various angles see Fig. 8). A standard reflection law is[47]

$$R(\theta) = \frac{R_0}{R_0 + (1-R_0)\cos^2(\theta)}. \tag{10}$$

Irregularities at the interface, e.g., a lattice constant mismatch or any kind of defects, will lead to some degree of diffuse scattering of quasiparticles at the grain boundaries. In order to model these irregularities we generalize Zaitsev's model to include interface roughness.[48] We model the grain boundary as a smooth interface coated on both sides with a thin dirty layer which scatters quasiparticles. The thin dirty layers are described by Ovchinnikov's model,[49] generalized to include elastic as well as inelastic scattering[50] at the grain boundaries.

The transport of quasiparticles across the dirty layers (DL's) is described by the transport equation[43]

$$\left[i\rho_{\rm in}\hat{\tau}_3 - \frac{\rho_0}{2\pi}\langle \hat{g}_{\rm DL}\rangle_{\pm}, \hat{g}_{\rm DL}\right] + ip_x\partial_x\hat{g}_{\rm DL} = 0, \quad 0 \leqslant |x| \leqslant 1, \tag{11}$$

where $\hat{g}_{\rm DL}$ is the quasiclassical propagator in the dirty layer. The second term in Eq. (11) is Ovchinnikov's elastic self-energy for incoming and reflected quasiparticles, whereas the first self-energy term, proportional to $\hat{\tau}_3$, models isotropic inelastic scattering. The propagators in the dirty layers are matched continuously to the propagators in the superconducting grains. The propagators are discontinuous at the smooth interface between the dirty layers, and the jump is given by Zaitsev's relations

$$\hat{d}_l = \hat{d}_r, \quad -i\pi\frac{1-R}{1+R}\left[\hat{s}_r\left(1-\frac{i}{2\pi}\hat{d}_r\right), \hat{s}_l\right] = \hat{d}_r(\hat{s}_r)^2, \tag{12}$$

where $\hat{d}_l$ ($\hat{d}_r$) and $\hat{s}_l$ ($\hat{s}_r$) are defined as the difference and the sum of the propagators in the dirty layer of the incoming and reflected particles on the left (right) side of the interface.

Our model for a grain boundary has three parameters: (1) a reflection probability R_0 for perpendicular incidence ($\theta = 0°$), (2) an elastic scattering rate ρ_0, and (3) an inelastic scattering rate $\rho_{\rm in}$. A quasiparticle hitting the grain boundary has a probability $R(\theta)$ to be reflected and a probability $1-R(\theta)$ to cross the grain boundary. The momentum parallel to the boundary is conserved for an ideal grain boundary ($\rho_0 = \rho_{\rm in} = 0$). Deviations from ideality are described by the elastic and inelastic scattering rates. Elastic scattering leads to pair breaking for superconductors with an anisotropic order parameter $\hat{\Delta}(\vec{p}_f)$, but not for an isotropic order parameter. Inelastic scattering is pair breaking for both. The scattering rates ρ_0 and $\rho_{\rm in}$ are assumed in the following to be independent of temperature because the normal resistances of single grain boundary junctions are reported to be independent of temperature.[16] A more detailed description of this model and a discussion of its physical consequences will be published elsewhere.[35]

In order to obtain the current-phase relationship across the interface we solve the quasiclassical differential equations self-consistently in the superconducting electrodes, subject to the matching condition across the interface obtained from our model. This gives us the self-consistent order parameter and the corresponding quasiclassical propagators. The calculations are done for a fixed phase difference of the order parameter across the junction, $\psi = \psi_r - \psi_l = \text{const}$. The critical-current density of the junction is then obtained via formula (9) as the maximum Josephson supercurrent density

$$j_{cJ}(T) = \max_{\psi} |j(\psi, T)|. \tag{13}$$

We emphasize that our model reproduces the Ambegaokar-Baratoff expression [Eq. (4)] and its generalization [Eq. (5)] for the Josephson critical current (1) for s-wave superconductors in the limit of weak transparency ($R_0 \approx 1$) and no inelastic scattering, and (2) in the limit of a smooth interface with weak transparency for d-wave superconductors with an interface oriented parallel to a crystal main axis.[38,46] In these cases there is no suppression of the order parameter, which would lead to deviations from the Ambegaokar-Baratoff result.

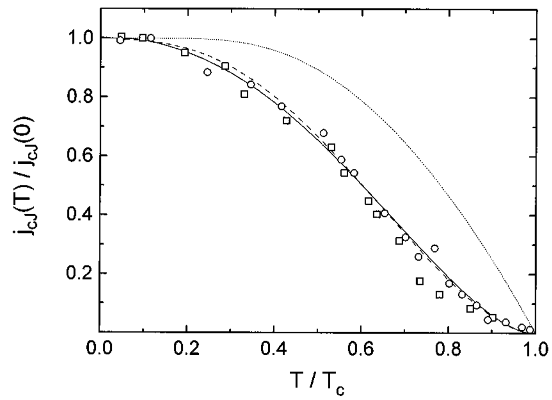

FIG. 9. Temperature dependence of the critical-current density of a symmetric single grain boundary junction. The experimental data are taken from Mannhart *et al.* (Ref. 51) [10° (□) and 15° (○) $YBa_2Cu_3O_{7-\delta}$ tilt boundary]. The solid (dashed) line is a theoretical curve obtained from our model for d-wave (s-wave) pairing with interface parameters $R_0 = 0.999$, $\rho_0 = 0.5$, $\rho_{\rm in} = 0$, $\alpha_l = 5°$, and $\alpha_r = -5°$ ($R_0 = 0.999$ and $\rho_{\rm in} = 0.17$). Dotted line: Ambegaokar-Baratoff behavior [Eq. (4)].

C. Numerical results and comparison with experiments

In Fig. 9 we compare temperature-dependent critical-current measurements on symmetric single grain boundary junctions by Mannhart *et al.*[51] (10° and 15° YBCO tilt boundaries) with our theoretical calculations. The experimental data are scanned from the original paper. We find excellent agreement between theory and experiment for d-wave as well as s-wave models. The optimum fit assuming d-wave pairing in the grains is obtained with $\rho_0 = 0.5$ and $\rho_{\rm in} = 0$. The theoretical data for $T < 0.05T_c$ are extrapolated data. Since the ratio of the critical-current density of the junctions and the depairing (Landau critical) current density at zero temperature is about 10^{-4}, we consider only weakly transparent interfaces with a reflection probability R_0 close to 1. For isotropic s-wave calculations, the elastic scattering rate ρ_0 does not influence the temperature dependence of j_c. The only possibility to fit the data in this case is to assume an unusually large inelastic scattering rate $\rho_{\rm in} = 0.17$. The essential effect responsible for the deviation of the temperature dependence of the Josephson critical current from the Ambegaokar-Baratoff behavior is the reduction of the order parameter at the boundary due to pair breaking effects. This effect is more pronounced at temperatures near T_c.

Our polycrystalline c-axis-oriented YBCO films consist of superconducting grains which are randomly oriented within the a-b plane. In order to compare our theoretical calculations on single junctions with our experiments we have to take into account this arbitrary orientation of the individual grains. Figure 10 shows the temperature dependence of the normalized intergranular critical-current density $j_{cJ}(T)/j_{cJ}(0)$ for the polycrystalline c-axis-oriented $YBa_2Cu_3O_{7-\delta}$ films as determined from $\chi''(h_{\rm ac})$ measurements and from transport measurements. As in the case for the single grain boundary junctions mentioned above, a quite good fit of the experimental data is obtained for s-wave pairing (dashed line) with reflection probability $R_0 = 0.999$ and an unusually large inelastic scattering rate $\rho_{\rm in} = 0.6$. In contrast to isotropic s-wave pairing there is an influence of the

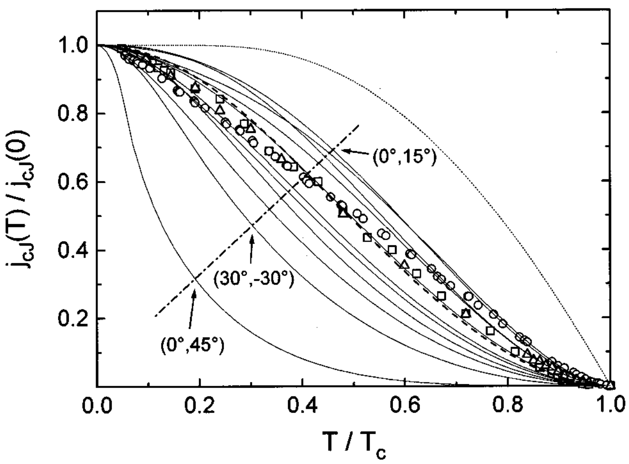

FIG. 10. Temperature dependence of the normalized intergranular critical-current density for our $YBa_2Cu_3O_{7-\delta}$ films as determined from $\chi''(h_{ac})$ measurements (□ and △) and from transport measurements (○). Solid lines: numerical calculations for single grain boundary junctions with several misorientation angles (α_l, α_r) of the two adjacent grains in case of d-wave pairing ($R_0=0.999$, $\rho_0=0.5$, $\rho_{in}=0$). Dashed line: s-wave pairing ($R_0=0.999$, $\rho_{in}=0.6$). Dotted line: Ambegaokar-Baratoff. For details see text.

misorientation angles α_l and α_r of the two adjacent grains on the critical current density for anisotropic d-wave pairing. The angles α_l (α_r) are defined as the angles between the normal of the interface layer and the a axis of the left (right) grain (cf. Fig. 8). The solid lines shown in Fig. 10 represent numerical results for different misorientation angles in case of d-wave pairing. From upper right to lower left the tilt angles along the dashed-dotted line are as follows: $(\alpha_l,\alpha_r)=$ (0°,15°), (0°,0°), (0°,30°), (15°,15°), (15°, 30°), (15°,45°), (30°,30°), (30°,45°), (45°,45°), (30°, −30°), and (0°,45°). The junction parameters are kept constant for all configurations ($R_0=0.999$, $\rho_0=0.5$, $\rho_{in}=0$). As can be argued from Fig. 10, a description of the behavior of our film by an effective junction model[52] would be accidental rather than systematic. Since the temperature dependences shown in Fig. 10 are similar for a wide range of misorientation angles with deviations only for angles close to 45°, it seems plausible that the measured temperature dependence of the intergranular critical-current density of our polycrystalline film can be modeled by a (complicated) interplay of individual single junctions. Such a model should include statistical methods as suggested, e.g., by Rhyner and Blatter,[53] who used the limiting path model which searches for the current limiting path in a two-dimensional array of randomly oriented grains arranged on a square lattice.

In contrast to the measured angle dependences of the critical current density in single grain boundary junctions (see Refs. 16,54–56, and references therein) which phenomenologically can be described by $j_{cJ}(\alpha)\approx j_{cJ}(0)\exp(-0.2\alpha)$ for $0°\leq\alpha\leq45°$ ($\alpha=\alpha_l-\alpha_r$), the calculated curves in Fig. 10 describe an intrinsic effect of d-wave pairing in the grains which is not caused by a varying quality or thickness of the junctions.

In this paper, we have restricted ourselves to the discussion of s-wave and d-wave pairing (see the Introduction). We have also carried out calculations for superconductors with anisotropic s-wave and extended s-wave pairing. While the data cannot be fitted by an anisotropic s-wave model, an extended s-wave symmetry of the order parameter leads to similar results as described in Fig. 10 for d-wave pairing.

V. SUMMARY

We have determined the temperature dependence of the intergranular critical current density j_{cJ} of polycrystalline, c-axis-oriented $YBa_2Cu_3O_{7-\delta}$ thin films at zero dc magnetic field from isothermal ac susceptibility $\chi(h_{ac})$ measurements. The obtained results have been compared with and confirmed by transport critical current measurements performed under self-field conditions. The measured temperature dependences deviate significantly from the Ambegaokar-Baratoff behavior, and are usually explained in terms of flux creep. In this paper, we have presented an alternative interpretation. Using a rather general model for interfaces, we have computed numerically the temperature dependence of the Josephson critical current across interfaces with arbitrary degree of transparency and roughness, including a self-consistent calculation of the order parameter in the vicinity of the boundary. Our theoretical results were compared (a) with measurements on single grain boundary junctions and (b) with our experiments on c-axis-oriented polycrystalline films. In both cases we have found excellent agreement between theory and experiment. We obtained significant deviations from the Ambegaokar-Baratoff behavior which can be understood by the depletion of the order parameter due to pair breaking effects at the interface. For d-wave symmetry of the pairing interaction in the grains this pair breaking is a natural consequence of the (diffuse) scattering of quasiparticles at the boundary which has no effect in isotropic superconductors. In order to explain the experimental data in case of isotropic s-wave pairing in the grains we had to take into account an unrealistically large inelastic scattering rate. Thus, we interpret the observed temperature dependences of the critical-current density as a consequence of Josephson tunneling between superconducting grains with d-wave symmetry.

ACKNOWLEDGMENTS

This work was supported by the Deutsche Forschungsgemeinschaft through SFB 279 (Wechselspiel zwischen Ordnung und Transport in Festkörpern). Parts of the SEM analyses have been performed at BIMF (Bayreuther Institut für Makromolekülforschung). We thank Clarissa Drummer for her assistance in the SEM analyses, Alexandra Krause and W. Ettig for technical assistance, C. Rogacki for his help and valuable hints concerning the contacting of the samples, M. Ziese for fruitful discussions, and D. W. Hess for a critical reading of the manuscript.

[1] B. G. Levi, Phys. Today **49**(1), 19 (1996); *ibid*. **46**(5), 17 (1993).

[2] D. J. Scalapino, Phys. Rep. **250**, 329 (1995).

[3] J. Annett, N. Goldenfeld, and A. J. Leggett, in *Physical Properties of High Temperature Superconductors V*, edited by D. M. Ginsberg (World Scientific, Singapore, in press).

[4] W. N. Hardy, D. A. Bonn, D. C. Morgan, R. Liang, and K. Zhang, Phys. Rev. Lett. **70**, 3999 (1993).

[5] Z. X. Shen, D. S. Dessau, B. O. Wells, D. M. King, W. E. Spicer, A. J. Arko, D. Marshall, L. W. Lombardo, A. Kapitulnik, P. Dickinson, S. Doniach, J. DiCarlo, A. G. Loeser, and C. H. Park, Phys. Rev. Lett. **70**, 1553 (1993).

[6] D. A. Wollman, D. J. Van Harlingen, W. C. Lee, D. M. Ginsberg, and A. J. Leggett, Phys. Rev. Lett. **71**, 2134 (1993).

[7] D. A. Wollman, D. J. Van Harlingen, J. Giapintzakis, and D. M. Ginsberg, Phys. Rev. Lett. **74**, 797 (1995).

[8] C. C. Tsuei, J. R. Kirtley, C. C. Chi, L. S. Yu-Jahnes, A. Gupta, T. Shaw, J. Z. Sun, and M. B. Ketchen, Phys. Rev. Lett. **73**, 593 (1994).

[9] J. R. Kirtley, C. C. Tsuei, J. Z. Sun, C. C. Chi, L. S. Yu-Jahnes, A. Gupta, M. Rupp, and M. B. Ketchen, Nature **373**, 225 (1995).

[10] A. G. Sun, D. A. Gajewski, M. B. Maple, and R. C. Dynes, Phys. Rev. Lett. **72**, 2267 (1994).

[11] V. Ambegaokar, P. G. deGennes, and D. Rainer, Phys. Rev. A **9**, 2676 (1974).

[12] J. R. Clem, Physica C **153-155**, 50 (1988).

[13] B. Renker, I. Apfelstedt, H. Küpfer, C. Politis, H. Rietschel, W. Schauer, H. Wühl, U. Gottwick, H. Kneissel, U. Rauchschwalbe, H. Spille, and F. Steglich, Z. Phys. B **67**, 1 (1987).

[14] J. W. C. De Vries, G. M. Stollman, and M. A. M. Gijs, Physica C **157**, 406 (1989).

[15] N. Savvides, Physica C **165**, 371 (1990).

[16] R. Gross, in *Interfaces in High-T_c Superconducting Systems*, edited by S. L. Shindé and D. A. Rudman (Springer, New York, 1994), p. 176.

[17] W. Widder, L. Bauernfeind, M. Stebani, and H. F. Braun, Physica C **249**, 78 (1995).

[18] J. H. Xu, J. L. Shen, J. H. Miller, Jr., and C. S. Ting, Phys. Rev. Lett. **73**, 2492 (1994).

[19] M. Tinkham, Helv. Phys. Acta **61**, 443 (1988); *Introduction to Superconductivity* (McGraw-Hill, New York, 1975).

[20] It was argued recently that the calculations of Xu contain an incorrect assumption (Refs. 57 and 58).

[21] F. Baudenbacher, K. Hirata, P. Berberich, and H. Kinder, J. Less Common Met. **164**, 269 (1990).

[22] M. Bauer (unpublished).

[23] T. R. Lemberger, in *Physical Properties of High Temperature Superconductors III*, edited by D. M. Ginsberg (World Scientific, Singapore, 1992), p. 471.

[24] R. Gross and B. Mayer, Physica C **180**, 235 (1991).

[25] J. R. Clem and A. Sanchez, Phys. Rev. B **50**, 9355 (1994).

[26] C. P. Bean, Phys. Rev. Lett. **250**, 8 (1962); Rev. Mod. Phys. **36**, 31 (1964).

[27] E. H. Brandt, Rep. Prog. Phys. **58**, 1465 (1995).

[28] M. F. Chisholm and S. J. Pennycook, Nature **351**, 47 (1991).

[29] D. Dimos, P. Chaudhari, J. Mannhart, and F. K. LeGoues, Phys. Rev. Lett. **61**, 219 (1988).

[30] M. Kawasaki, P. Chaudhari, and A. Gupta, Phys. Rev. Lett. **68**, 1065 (1992).

[31] D. Winkler, Y. M. Zhang, P. Å. Nilsson, E. A. Stepantsov, and T. Claeson, Phys. Rev. Lett. **72**, 1260 (1994).

[32] T. Doderer, Y. M. Zhang, D. Winkler, and R. Gross, Phys. Rev. B **52**, 93 (1995).

[33] V. Ambegaokar and A. Baratoff, Phys. Rev. Lett. **10**, 486 (1963); **11**, 104(E) (1963).

[34] Taking into account the anisotropy of the superconducting order parameters on both sides of the junction, a calculation analogous to that of Ref. 33 by Ambegaokar and Baratoff leads to Eq. (5), which reduces to $I_s=(eR_N)^{-1}\Delta_1(T)\Delta_2(T)\pi k_B T\Sigma_{n=0,\pm 1,\ldots}\{[\epsilon_n^2+\Delta_1^2(T)][\epsilon_n^2+\Delta_2^2(T)]\}^{-1/2}$ given in Ref. 33 for isotropic order parameters Δ_1 and Δ_2, where $R_N^{-1}=4\pi e^2 N_f^l N_f^r \langle\langle|T_{\vec{p}_f^l\vec{p}_f^r}|^2\rangle_{\vec{p}_f^l}\rangle_{\vec{p}_f^r}$.

[35] H. Burkhardt *et al.* (unpublished).

[36] L. J. Buchholtz, M. Palumbo, D. Rainer, and J. A. Sauls, J. Low Temp. Phys. **101**, 1079 (1995).

[37] L. J. Buchholtz, M. Palumbo, D. Rainer, and J. A. Sauls, J. Low Temp. Phys. **101**, 1099 (1995).

[38] Yu. S. Barash, A. V. Galaktionov, and A. D. Zaikin, Phys. Rev. B **52**, 665 (1995).

[39] A smooth interface conserves the parallel component of the quasiparticle momentum.

[40] G. Eilenberger, Z. Phys. **214**, 195 (1968).

[41] A. I. Larkin and Yu. N. Ovchinnikov, Zh. Eksp. Teor. Fiz. **55**, 2262 (1968) [Sov. Phys. JETP **28**, 1200 (1969)].

[42] A. V. Zaitsev, Zh. Eksp. Teor. Fiz. **86**, 1742 (1984) [Sov. Phys. JETP **59**, 1015 (1984)].

[43] F. J. Culetto, G. Kieselmann, and D. Rainer, in *Proceedings of the 17th International Conference on Low Temperature Physics*, edited by U. Eckern, A. Schmid, W. Weber, and H. Wühl (North-Holland, Amsterdam, 1984), p. 1027.

[44] B. Ashauer, G. Kieselmann, and D. Rainer, J. Low Temp. Phys. **63**, 349 (1986).

[45] J. Kurkijärvi, D. Rainer, and J. A. Sauls, Can. J. Phys. **65**, 1440 (1987).

[46] A. Millis, D. Rainer, and J. A. Sauls, Phys. Rev. B **38**, 4504 (1988).

[47] G. Kieselmann, Phys. Rev. B **35**, 6762 (1987).

[48] J. A. Sauls (private communication).

[49] Yu. N. Ovchinnikov, Zh. Eksp. Teor. Fiz. **56**, 1590 (1969) [Sov. Phys. JETP **29**, 853 (1969)].

[50] The term ''inelastic'' refers here to pair breaking scattering processes such as inelastic scattering, magnetic scattering, etc.

[51] J. Mannhart, P. Chaudhari, D. Dimos, C. C. Tsuei, and T. R. McGuire, Phys. Rev. Lett. **61**, 2476 (1988).

[52] In an effective junction model the behavior of the complicated network can be reduced on the behavior of a single junction with an effective misorientation angle α_{eff}.

[53] J. Rhyner and G. Blatter, Phys. Rev. B **40**, 829 (1989).

[54] D. Dimos, P. Chaudhari, and J. Mannhart, Phys. Rev. B **41**, 4038 (1990).

[55] J. Alarco, Y. Boikov, G. Brorsson, T. Claeson, G. Daalmans, J. Edstam, Z. Ivanov, V. K. Kaplunenko, P. Å. Nilsson, E. Olsson, H. K. Olsson, J. Ramos, E. Stepantsov, A. Tzalenchuk, D. Winkler, and Y. M. Zhang, in *Materials and Crystallographic Aspects of HT_c-Superconductivity*, edited by E. Kaldis (Kluwer Academic Publishers, Dordrecht, 1994), p. 471.

[56] H. Hilgenkamp, J. Mannhart, and B. Mayer, Phys. Rev. B **53**, 14 586 (1996).

[57] Yu. S. Barash, A. V. Galaktionov, and A. D. Zaikin, Phys. Rev. Lett. **75**, 1676 (1995).

[58] C. Bruder, A. van Otterlo, and G. T. Zimanyi, Phys. Rev. B **51**, 12 904 (1995).